Vol 16 No 3, March 2007
1009-1963/2007/16(03)/0740-06
Chinese Physics
© 2007 Chin. Phys. Soc.
and IOP Publishing Ltd

Steering light into logic patterns with two-dimensional cascaded multimode waveguide*

Zhou Hai-Feng(周海峰), Yang Jian-Yi(杨建义),
Wang Ming-Hua(王明华), and Jiang Xiao-Qing(江晓清)†

Department of Information Science and Electronics Engineering, Zhejiang University, Hangzhou 310027*, China*

(Received 11 April 2006; revised manuscript received 12 September 2006)

Steering light into logic patterns with two-dimensional cascaded multimode waveguide is demonstrated. By employing the imaging properties of 2D multimode interference (MMI) and partial phase modulation method, the design ideas and the implementing methods of the $2^{(2\times2)}$ bits type spatial logic steering are discussed; therefore the structure of logical pattern is proposed. Numerical simulation is carried out to verify the design in detail by using the beam propagation method. It is expected to realize logic coders by using the integrated optical methods and exploit their potential applications in the field of optical logic.

Keywords: integrated optics, multimode interference, spatial light modulators, logic patterns
PACC: 4282, 4280L

1. Introduction

Optical information processing demands compact and high-capacity photonics devices. Functional devices including spatial light modulator,[1] 3D directional couplers[2] and 2D wavelength (de) multiplexer[3] have flourished enormously over the past decades, with no exception of optical logic devices, especially logic gates and coders. Optical logic gates by using semiconductor optical amplifiers (SOA),[4,5] thermal lens effect,[6] bacteriorhodopsin film[7] and optical pulse in SiGe/Si multimode interference (MMI)[8] have been reported. Simultaneously, optical encoder based on Moiré effect and fractional Talbot self-image effect of gratings[9] also appeared in previous publications. Most of them are based on the micro-optical method and always supported by lots of mechanical equipments. Using integrated optical structures to design encoders can evade these problems and shows great promise. Here we use MMI structures to steer light into logic patterns and pave the way for realizing integrated optical coders.

MMI devices have gained widespread application due to their excellent properties,[10] in constructing splitters and switches,[10] mode converters,[11] phase (de) multiplex[12] and optical logic gates.[8] Based on multimode waveguides, this paper is to present a logic coder switch, which steers light into logic patterns with a 2D cascaded multimode waveguide with the partial phase modulation.[13] Based on the fundamental principle of 2D MMI, we analyze the operation mechanism of the $2^{(2\times2)}$ bits spatial logic steering. All the design results are simulated by using the finite difference beam propagation method (BPM). With self-imaging characterizations, the MMI device has a good rebuilding function and holds steady and uniform output beam shapes, so it is easy-to-cascade and reliable. The proposed structure employs partial phase modulation to obtain controllable fan-outs, and all the light energy can efficiently pass through the device in contrast to the amplitude-type devices.

To meet the needs of high integration level with dense channels per chip and reduced chip size, fabrication techniques to the 2nd or 3rd dimension have developed rapidly. Sun *et al* [14] have experimentally demonstrated 2D MMI power splitters based on Silicon on insulator (SOI). Wächter *et al* [15,16] have investigated different technological schemes. These progresses help us realize the proposed structure.

2. Principle and analysis

2D $(M \times N) \times (M \times N)$ MMI is obtained by extending the 1D confinement MMI, which can be explained explicitly through the guide-mode propaga-

*Project supported by the National Natural Science Foundation of China (Grant No 60477018) and the Major Program of the National Natural Science Foundation of China (Grant No 60436020).
†E-mail: iseejxq@zju.edu.cn

tion theory.[10] Jiang *et al*[17] and Sun *et al*[18] obtained the general and overlapping imaging properties and found that the self-imaging effect in 2D MMI could be regarded as the superposition coupling of two orthogonal and independent one-dimensional self-imaging effects. For 2D $(M \times N) \times (M \times N)$ MMI, the output transverse field at a distance $z = L$ can be written as

$$f_{\text{out}}(x, y, L) = \frac{1}{C(L)} \sum_{m=1}^{M} \sum_{n=1}^{N} f_{\text{in}}(x - x_m, y - y_n, 0) \times \exp(\text{j}\theta_m + \text{j}\theta_n), \quad (1)$$

where $C(L)$ is the complex normalization constant; x_m, y_n, and θ_m, θ_n are the relative positions and phases of the images (the mth in the x-direction and the nth in the y-direction), respectively. f_{in} is the input field distribution extended to some virtual sections periodically. The expression above indicates that we can evaluate the output field distribution by laterally translating the coordinates of the input field to compose the $M \times N$ output images. In other words, the field of each output is the coherent superposition of all the component fields from the $M \times N$ input ports. Thus, the relations between the outputs and the inputs can be described more intuitively and generally than Eq.(1) by

$$R_l \exp(\text{j}\psi_l) = \sum_{k=1}^{M \times N} r_{kl} \exp(\text{j}\varphi_{kl}) \cdot R_k \exp(\text{j}\psi_k), \quad (2)$$

where r_{kl} and φ_{kl} are the transmission coefficient and the relative phase of the input k, respectively, contributing to the output $l (k, l = 1, \ldots, M \times N)$. R_l and ψ_l are correspondent to the finally combined field of the output port l. The field of each output depends on all the inputs and the transmission process. In particular, if the values of r_{kl} have an equal value for all k and l pairs, the superposition only depends on the phase relations. This discursion roots in the law of causation.

With relation to multi-level cascaded MMI (e.g. n MMI connected by $n-1$ modulation regions), we can use transfer matrix method to explain this system.[19] The factor $r_{kl}\ \exp(\text{j}\varphi_{kl})$ in expression (2) can form a matrix S_{MMI} with $M \times N$ rows and $M \times N$ columns, where subscripts k and l represent the row and column numbers, respectively. The phase shifts in the modulating regions can be described by a diagonal matrix S_{MR} (i.e. $\exp[\text{j} \cdot \text{diag}(\delta\varphi_1, \delta\varphi_2, \ldots, \delta\varphi_{M\times N})]$.) as follows:

$$S_{\text{MMI}} = \begin{pmatrix} r_{11}\exp(\text{j}\varphi_{11}) & r_{12}\exp(\text{j}\varphi_{12}) & \cdots & r_{1,M\times N}\exp(\text{j}\varphi_{1,M\times N}) \\ r_{21}\exp(\text{j}\varphi_{21}) & r_{22}\exp(\text{j}\varphi_{22}) & \cdots & r_{2,M\times N}\exp(\text{j}\varphi_{2,M\times N}) \\ \cdots & \cdots & \cdots & \cdots \\ r_{M\times N,1}\exp(\text{j}\varphi_{M\times N,1}) & r_{M\times N,2}\exp(\text{j}\varphi_{M\times N,2}) & \cdots & r_{M\times N,M\times N}\exp(\text{j}\varphi_{M\times N,M\times N}) \end{pmatrix}_{M\times N, M\times N}, \quad (3)$$

$$S_{\text{MR}} = \exp[\text{j} \cdot \text{diag}(\delta_1, \delta_2, \cdots, \delta_{M\times N})] = \exp\left[\text{j} \begin{pmatrix} \delta\varphi_1 & & & \\ & \delta\varphi_2 & & \\ & & \ddots & \\ & & & \delta\varphi_{M\times N} \end{pmatrix}_{M\times N, M\times N}\right]. \quad (4)$$

Thus, the input/output transfer matrix for analysing the cascaded MMI system can be expressed as

$$T = S_{\text{MMI}} \cdot S_{\text{MR},n-1} \times \cdots \times S_{\text{MMI}} \cdot S_{\text{MR},1} \cdot S_{\text{MMI}}. \quad (5)$$

Based on the fundamental principles of the 2D $(2\times2)\times(2\times2)$ MMI cell (see Fig.1), we analyze the inherent operation mechanism of the $2^{(2\times2)}$ spatial logic steering. Denote two outputs with the intensity ratio higher than 9:1 (i.e. $>$ 9.5 dB) as 'ON' and 'OFF' logic states, respectively. Consider two outputs with the intensity difference less than 1% of total intensity as being in the same state. Here our goal is to realize 16 logic states with the four outputs of 2D (2×2)

× (2×2) MMI by employing the difference partial phase modulation method. The centre of the four inputs and their corresponding outputs, which are numbered '1', '2', '3' and '4', are located symmetrically at $(W_e/3, W_e/3)$, $(2W_e/3, W_e/3)$, $(W_e/3, 2W_e/3)$ and $(2W_e/3, 2W_e/3)$, respectively. Both the x- and y- directions satisfy the overlapping imaging conditions.[16] When $L_{mmi} = L_\pi/2 = 2n_c W_e^2/3\lambda_0$, each input produces four uniform-intensity images at the outputs. Here, W_e is the effective width of the multimode waveguide, n_c is the waveguide index, and λ_0 is the operation wavelength in vacuum. The relative phase relations between the inputs and the outputs are listed in Table 1. For $r_{kl} = 1/2$, S_{MMI} can be determined.

Table 1. Relative phases of 2D $(2\times2)\times(2\times2)$ MMI coupler.

Phase ϕ_{kl}	$k=1$	$k=2$	$k=3$	$k=4$
$l=1$	0	$\pi/2$	$\pi/2$	π
$l=2$	$\pi/2$	0	π	$\pi/2$
$l=3$	$\pi/2$	π	0	$\pi/2$
$l=4$	π	$\pi/2$	$\pi/2$	0

Feed the four inputs together with $(I_1^{in}, \varphi_1^{in})$, $(I_2^{in}, \varphi_2^{in})$, $(I_3^{in}, \varphi_3^{in})$ and $(I_4^{in}, \varphi_4^{in})$, correspondingly. In view of the formula (2), the images from all the inputs interfere with each other at each output port. The output intensity of the l port can be evaluated by

$$I_l^{out} = |R_l^{out}\exp(j\psi_l^{out})|^2. \tag{6}$$

Take output port '1' as example, its optical field can be expressed as

$$R_l^{out}\exp(j\psi_l^{out})|_{l=1} = \sum_{k=1}^{4} r_{k1}\exp(j\varphi_{k1})\cdot R_k^{in}\exp(j\psi_k^{in})$$
$$= \frac{\sqrt{I_1^{in}}}{2}\exp(j\psi_1^{in}) + \frac{\sqrt{I_2^{in}}}{2}\exp\left[j\left(\psi_2^{in}+\frac{\pi}{2}\right)\right]$$
$$+ \frac{\sqrt{I_3^{in}}}{2}\exp\left[j\left(\psi_3^{in}+\frac{\pi}{2}\right)\right]$$
$$+ \frac{\sqrt{I_4^{in}}}{2}\exp\left[j(\psi_4^{in}+\pi)\right]. \tag{7}$$

Likewise, similar expressions of the other three outputs can be obtained. Thus, changing the input intensities and phases can produce a series of available output intensity distributions. By assuming the total intensity $I_{total} = I_1^{in} + I_2^{in} + I_3^{in} + I_4^{in} = 1$, various relative intensity distribution patterns can be obtained. If four inputs have the same intensity but different phases, all possible states with one, two and four 'ON' states in connection to the essential output patterns (2)–(5) in Table 2 can be obtained.

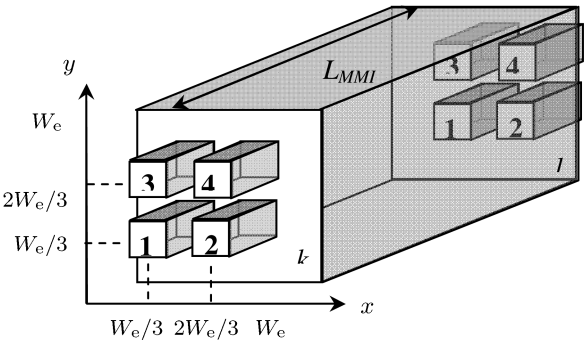


Fig.1. The unit component of the coder switch, 2D $(2\times2)\times(2\times2)$ MMI, where changing the input intensity and phase can obtain various output patterns.

Table 2. Essential output patterns obtained by changing the input intensities and phases.

Essential output patterns	Input intensity and phase distribution $\begin{pmatrix}(I_3^{in},\psi_3^{in}) & (I_4^{in},\psi_4^{in})\\(I_1^{in},\psi_1^{in}) & (I_2^{in},\psi_2^{in})\end{pmatrix}$	Output intensity distribution $\begin{pmatrix}I_3^{out} & I_4^{out}\\I_1^{out} & I_2^{out}\end{pmatrix}$	Logic representation & Remarks
(1)	$\begin{pmatrix}(0,0) & (0,0)\\(1,\text{arbitrary}) & (0,0)\end{pmatrix}$	$\begin{pmatrix}0.25 & 0.25\\0.25 & 0.25\end{pmatrix}$	For input section
(2)	$\begin{pmatrix}(0.25,\pi/2) & (0.25,\pi)\\(0.25,0) & (0.25,\pi/2)\end{pmatrix}$	$\begin{pmatrix}0 & 1\\0 & 0\end{pmatrix}$	$\begin{bmatrix}0 & 1\\0 & 0\end{bmatrix}$
(3)	$\begin{pmatrix}(0.25,\pi/2) & (0.25,\pi/2)\\(0.25,0) & (0.25,0)\end{pmatrix}$	$\begin{pmatrix}0.5 & 0.5\\0 & 0\end{pmatrix}$	$\begin{bmatrix}1 & 1\\0 & 0\end{bmatrix}$
(4)	$\begin{pmatrix}(0.25,0) & (0.25,0)\\(0.25,\pi) & (0.25,0)\end{pmatrix}$	$\begin{pmatrix}0 & 0.5\\0.5 & 0\end{pmatrix}$	$\begin{bmatrix}0 & 1\\1 & 0\end{bmatrix}$
(5)	$\begin{pmatrix}(0.25,0) & (0.25,0)\\(0.25,0) & (0.25,0)\end{pmatrix}$	$\begin{pmatrix}0.25 & 0.25\\0.25 & 0.25\end{pmatrix}$	$\begin{bmatrix}1 & 1\\1 & 1\end{bmatrix}$

However, the three 'ON' states cannot be achieved until we set the input intensities to be unequal. That is to say, four inputs with equal intensity and any phase combination cannot produce three uniform-intensity outputs through one single MMI section (SC), which can be proven strictly with Eq.(2). Fortunately, we can form a primary optical field with a certain intensity ratio e.g. 1:1:1:5 through one MMI SC for the first step. After modulating the phases, finally we can obtain an extremely approximate distribution of the three 'ON' case through another MMI SC for the second step (in Table 3).

Table 3. Two steps for the realization of three 'ON' and one 'OFF' states.

First step	$\begin{pmatrix} (0.25,0) & (0.25,\pi/2) \\ (0.25,0) & (0.25,0) \end{pmatrix}$	$\begin{pmatrix} 0.125 & 0.625 \\ 0.125 & 0.125 \end{pmatrix}$	Intensity ratio (1:1:1:5)
Second step	$\begin{pmatrix} (0.125,\pi/4) & (0.625,-\pi/4) \\ (0.125,-\pi/4) & (0.125,\pi/4) \end{pmatrix}$	$\begin{pmatrix} 0.3273 & 0.0182 \\ 0.3273 & 0.3273 \end{pmatrix}$	$\begin{bmatrix} 1 & 0 \\ 1 & 1 \end{bmatrix}$

3. Configuration and simulation

With the MMI cell above, we propose the configuration consisting of three cascaded MMI SCs connected by two modulation regions (MRs) to construct the $2^{(2\times2)}$ spatial logic states (Fig.2). This system functions as $T = S_{\mathrm{MMI}}S_{\mathrm{MR},2}S_{\mathrm{MMI}}S_{\mathrm{MR},1}S_{\mathrm{MMI}}$.The light from arbitrary single input port uniformly splits its intensity into the MR1 through the SC1; after modulating the phases (i.e., supplementing appropriate phase differences or not, which are listed in Table 4, to satisfy the required input phase condition of the MMI SC2) in MR1 and propagating through SC2 into MR2, the primarily required uniform or non-uniform (e.g. 1:1:1:5) field can be obtained in front of the MR2; with additional phase modulations in the MR2 and propagation in the SC3, the final mode profiles can be formed.

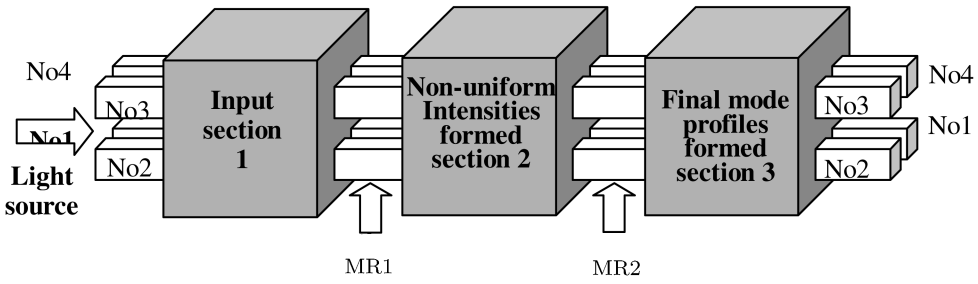


Fig.2. The proposed configuration of the spatial logic coder based on 2D (2×2)×(2×2) MMI, which consists of three cascaded MMI connected by two modulation regions.

Table 4. The mapping relation between the phase modulations and Boolean logic states. The first matrices in Table 4 (a–c) are corresponding to the simulation results in Fig.3.

Figure number	$\{\delta\varphi_1,\delta\varphi_2,\delta\varphi_3,\delta\varphi_4\}_{\mathrm{MR},1}$	Primary field distribution	$\{\delta\varphi_1,\delta\varphi_2,\delta\varphi_3,\delta\varphi_4\}_{\mathrm{MR},2}$	$\begin{bmatrix} \text{No 3} & \text{No 4} \\ \text{No 1} & \text{No 2} \end{bmatrix}$ Boolean logic states
a	$\{0,3\pi/2,3\pi/2,\pi\}$	1:1:1:1	$\{0,\pi/2,\pi/2,\pi\}$	$\begin{bmatrix} 0 & 1 \\ 0 & 0 \end{bmatrix}\begin{bmatrix} 0 & 0 \\ 1 & 0 \end{bmatrix}\begin{bmatrix} 0 & 0 \\ 0 & 1 \end{bmatrix}\begin{bmatrix} 1 & 0 \\ 0 & 0 \end{bmatrix}$
b	$\{0,3\pi/2,3\pi/2,\pi\}$	1:1:1:1	$\{0,0,\pi/2,\pi/2\}$	$\begin{bmatrix} 1 & 1 \\ 0 & 0 \end{bmatrix}\begin{bmatrix} 0 & 0 \\ 1 & 1 \end{bmatrix}\begin{bmatrix} 1 & 0 \\ 1 & 0 \end{bmatrix}\begin{bmatrix} 0 & 1 \\ 0 & 1 \end{bmatrix}$
c	$\{0,3\pi/2,3\pi/2,\pi\}$	1:1:1:1	$\{\pi,0,0,0\}$ or $\{0,\pi,\pi,\pi\}$	$\begin{bmatrix} 0 & 1 \\ 1 & 0 \end{bmatrix}\begin{bmatrix} 1 & 0 \\ 0 & 1 \end{bmatrix}$
d	No modulation	0:0:0:1	No modulation	$\begin{bmatrix} 1 & 1 \\ 1 & 1 \end{bmatrix}$
e	$\{0,0,0,3\pi/2\}$	1:1:1:5	$\{\pi,0,0,\pi/2\}$	$\begin{bmatrix} 1 & 0 \\ 1 & 1 \end{bmatrix}\begin{bmatrix} 1 & 1 \\ 1 & 0 \end{bmatrix}\begin{bmatrix} 0 & 1 \\ 1 & 1 \end{bmatrix}\begin{bmatrix} 1 & 1 \\ 0 & 1 \end{bmatrix}$

Silicon-on-glass materials are chosen to exemplify the device, with the core index n_c being 3.45 for silicon and the substrate index n_s being 1.51 for glass. Assume operation wavelength $\lambda_0 = 1.55$ μm. The widths W_e of the square cross sections of the MMI SCs are 12.16 μm. Thus,

$$L_{MMI} = 218 \ \mu\text{m}.$$

The lengths of 8 identical connecting guides in two MRs are all 22.46 μm so as to obtain a phase change of π for a refractive index change of 1%. Both the widths and the heights of all the input/output and connecting waveguides are 2 μm.

By performing the simulation with BPM Software based on the 3D finite-difference beam propagation method, we obtain all correspondent output patterns of the logic Boolean states in Fig.3, which is in good agreement with theoretical calculation. Let the initial input port be numbered '1'. All the phase modulation and implementation of Boolean logic states are listed in Table 4.

Figure 3 lists five typical logic outputs as an example corresponding to the grey matrices in the five different categories in Table 4. For example, the incident beam uniformly splits into the four waveguides in the MR1 with the relative phase distribution $[0, \pi/2, \pi/2, \pi]^{\mathrm{T}}$; if modulating $\{\delta\varphi_1, \delta\varphi_2, \delta\varphi_3, \delta\varphi_4\}_{\mathrm{MR},1}$ in the MR1 with a phase difference $\{0, 3\pi/2, 3\pi/2, \pi\}$ so as to obtain the initial phase $[0, 0, 0, 0]^{\mathrm{T}}$ in the SC2, the four ports in front of the MR2 can collect the uniform intensity and common phases again; then modulating $\{\delta\varphi_1, \delta\varphi_2, \delta\varphi_3, \delta\varphi_4\}_{\mathrm{MR},2}$ in the MR2 with a phase difference $\{0, \pi/2, \pi/2, \pi\}$, the final field distribution in Fig.3(a) can be obtained, which denotes the Boolean logic state $\left[\begin{smallmatrix} 0 & 1 \\ 0 & 0 \end{smallmatrix}\right]$. According to the rotational symmetry, the other three states of the first category in Table 4(a): $\left[\begin{smallmatrix} 0 & 0 \\ 1 & 0 \end{smallmatrix}\right]$, $\left[\begin{smallmatrix} 0 & 0 \\ 0 & 1 \end{smallmatrix}\right]$ and $\left[\begin{smallmatrix} 1 & 0 \\ 0 & 0 \end{smallmatrix}\right]$, can be realized with the similar phase modulations $\{\pi, \pi/2, \pi/2, 0\}$, $\{\pi/2, \pi, 0, \pi/2\}$, $\{\pi/2, 0, \pi, \pi/2\}$ in the MR2, respectively.

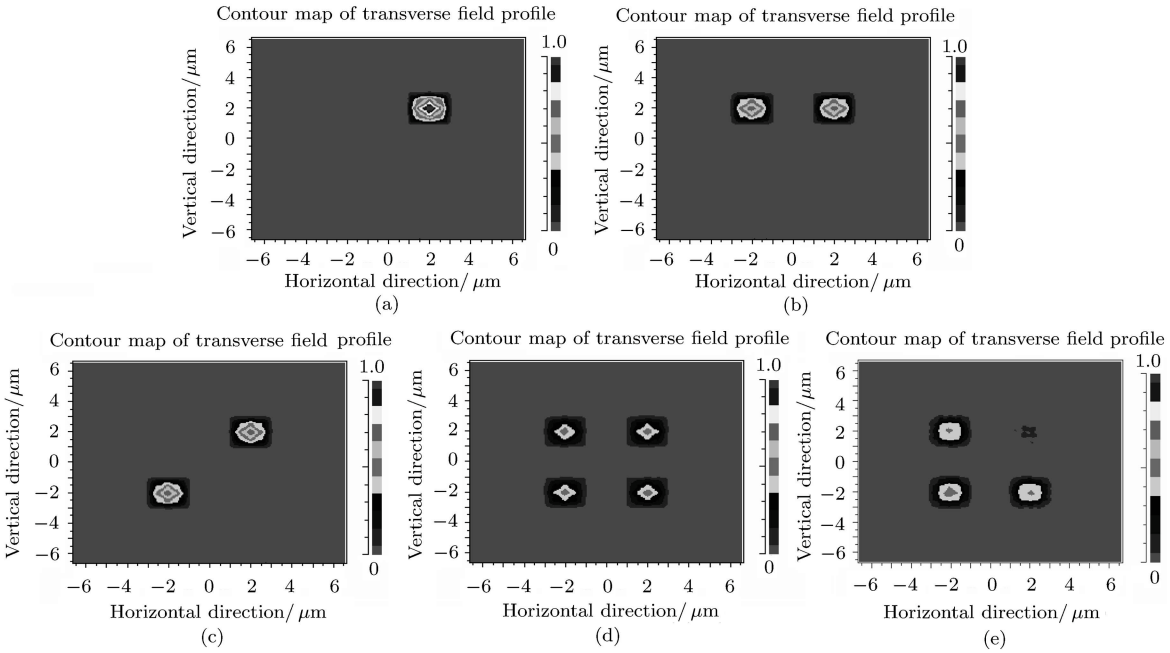


Fig.3. Five typical logic outputs with different phase modulations corresponding to the five grey matrices in the five different categories in Table 4.

In Table 4 and Fig.3, some features should be discussed and explained. First, in each MR region, one of the four modulating ports can be theoretically cancelled through adjusting the phases of the other three ports because only the relative phases are concerned. For example, in order to keep '1' non-modulated in the MR2, the output pattern in Fig.3(c) can also be implemented by replacing $(\pi, 0, 0, 0)$ with its equivalent $(0, \pi, \pi, \pi)$. Second, no input produces the all 'OFF' state $\left[\begin{smallmatrix} 0 & 0 \\ 0 & 0 \end{smallmatrix}\right]$, which is not included in Table 4. Third, theoretically, the perfect imaging patterns with infinitely high extinction ratios can form to express the eleven Boolean logic states included in Figs.3(a–d), but the other four states in Fig.3(e) are expressed

approximately but not strictly by the imaging patterns. The extinction ratio between the 'ON' and 'OFF' states theoretically reaches 12.36dB that is reliable and clear enough to constitute the logic patterns.

More pertinent problems about the device have been investigated. Most of the merits possessed by MMI still hold true in this device. Because of the rotational symmetry in the x- and y- directions, the device based on square MMIs can reasonably be expected to be insensitive to polarization.[20] Compared with the MMI length, the transverse size should be controlled rigorously. The acceptable bandwidth of this device is about 10 nm. The coupling among the four guides in the short MRs is so weak for strongly confined materials that the power exchange may be ignored. Additional scattering losses introduced by the change of refractive index in the MRs may partly deteriorate the uniformity of the imaging spots in the experimental fabrication.

$M \times N$ input/output arrays can theoretically be generalized to steer $2^{(N\times M)}$ bits logic patterns with large M and N. But, some states, e.g. the three 'ON' states for $2^{(2\times 2)}$ type here, cannot be strictly obtained, which require more sections to implement these states gradually and the realization approach is very flexible but uneasy to determine systematically. Increasing the values of M and N will obviously blur the images, and result in a lower extinction ratio and high propagation loss.

In spite of the rotational symmetry of the proposed structure, when one input port is mapped into one logic pattern at a certain phase modulation, other three inputs are mapped into nothing (e.g. when $\{\delta\varphi_1, \delta\varphi_2, \delta\varphi_3, \delta\varphi_4\}_{\mathrm{MR},1} = \{0, 0, 0, 3\pi/2\}$ and $\{\delta\varphi_1, \delta\varphi_2, \delta\varphi_3,\ \delta\varphi_4\}_{\mathrm{MR},2} = \{\pi, 0, 0, \pi/2\}$, an excited beam from port 1 produces three 'ON' states, but no Boolean state can be obtained with the beam excited from port 2). Without the compatibility it will be complicated to modulate the phase. These points present us a new research subject.

4. Conclusions

In summary, we have numerically investigated the logic behaviour of cascaded 2D multimode waveguides. This paper has proposed the $2^{(2\times 2)}$ bits spatial optical logic steering based on 2D MMI with partial phase modulation. 16 logic patterns are obtained with different phase modulations. Although improvements should be made for some details, our studies fully embody some advantages of 2D integration including rather compact size and the enhanced transmission capacitance. The present work is mainly devoted to exhibiting the design scheme. How to modulate the phase accurately and fabricate the 3D structure seems to be a challenging research subject.

References

[1] Noguchi K 1998 *J. Lightwave Technol.* **16** 1473

[2] Friedrich L, Dannberg P, Wachter D, Henning T, Brauer A and Karthe W 1997 *Opt. Commun.* **137** 239

[3] Yang J Y, Jiang X Q, Wang M H and Wang Y L 2004 *Opt. Exp.* **12** 1084

[4] MeAulay A D 2002 in *Photonic Devices and Algorithms for Computing* IV *Proc. SPIE* **4788** 83

[5] Wang Y, Zhang X L and Huang D X 2004 *Chin. Phys.* **13** 882

[6] Kurian A, Unnikrishnan K P, Gopinath P, Paul B, Nampoori V P N and Vallabhan C P G 2001 in *Photonic Systems and Applications Proc. SPIE* **4595** 100

[7] Chen G Y, Zhang C P, Guo Z X, Tian J G, Zhang G Y and Song Q W 2005 *Chin. Phys.* **14** 774

[8] Li Z J, Chen Z W and Li B J 2005 *Opt. Exp.* **13** 1033

[9] Kao C F and Lu M H 2005 *Opt. Commun.* **250** 16

[10] Soldano L B and Pennings E C M 1995 *J. Lightwave Technol.* **13** 615

[11] Leeuthold J, Eckner J, Gamper E, Besse P A and Melchior H 1998 *J. Lightwave Technol.* **16** 1228

[12] Yehia A and Khalil D 2005 *J. Sel. Top. Quantum Electron.* **11** 444

[13] Yagi M, Nagai S, Inayoshi H and Utaka K 2000 *Electron. Lett.* **36** 533

[14] Sun Y L, Jiang X Q, Yang J Y, Tang Y and Wang M H 2003 *Chin. Phys. Lett.* **20** 2182

[15] Wächter C, Hennig T, Bauer T, Bräuer A and Karthe W 1998 *Proc. SPIE* **3278** 102

[16] Wäechter C, Bauer T, Cumme M, Kannberg P, Elflein W, Hennig T, Streppel U and Karthe W 2000 *Proc. SPIE* **3936** 130

[17] Jiang X Q, Mao H L and Wang M H 2002 *Proc. SPIE* **4904** 51

[18] Sun Y L, Jiang X Q, Yang J Y and Wang M H 2005 *Chin. Opt. Lett.* **3** 154

[19] Lagali N S, Paiam M R and MacDonald R I 1999 *IEEE Photon. Technol. Lett.* **11** 665

[20] Chen H and Tong D T K 2005 *IEEE Photon. Technol. Lett.* **17** 801